



DOI: 10.18720/MCE.87.9

Efficacy of digital elevation and Nash models in runoff forecast

D.V. Kozlov*, A.A. Ghebrehiwot,

National Research Moscow State Civil Engineering University, Moscow, Russia

* *E-mail: kozlovdv@mail.ru*

Keywords: digital elevation model, QGIS algorithm, GIUH-Nash model, direct surface runoff, hydrograph, catchment, river network, runoff forecast.

Abstract. Digital elevation models (DEMs) are extensively used in hydrological modelling and deriving the geomorphological properties of catchments. Recently, hydrologists have shown interest in researching the effects of DEMs from different sources on simulated outputs. As part of these efforts, this study aimed at evaluating the effects of DEM and algorithm selection on geomorphologic instantaneous unit hydrographs (GIUH)-Nash model based direct surface runoff predictions from ungauged Debarwa river catchment in Eritrea. Four open-source DEMs and two quantum geographic information system (QGIS) algorithms (GRASS and SAGA) were applied and corresponding outputs were evaluated using five observed events. The two algorithms resulted in drainage networks of similar stream orders but different geomorphologic characteristics such as stream ratios. The subjective and objective goodness of fit results indicated that the performance of the model based on SAGA was unsatisfactory whereas that of GRASS algorithm-based GIUH-Nash model was acceptable for all the DEM-scenarios irrespective of their sources and resolutions. The study concluded that DEM in the calculation of flow hydrographs for the conditions of the Debarwa catchment selection has little impact on the GIUH-Nash model based direct surface runoff predictions and can be used indiscriminately. But, great care should be taken while selecting stream network generating algorithms, especially for catchments whose outlets are located near the confluence of two major rivers.

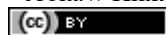
1. Introduction

The State of Eritrea is located on east coast of Africa between 12°22' and 18°02' N latitude and 36°26' and 43°13' E longitude and includes the Dahlak archipelago and other islands along the Red Sea coast. It is bordered by Sudan in the north and west, Ethiopia in the south, Djibouti in the south-east and the Red Sea in the north and north-east. It covers an area of 124, 320 km² comprising high plateaus and plains. Prior to its independence in 1993, Eritrea was a colony of Turkey, Egypt, Italy, British and Ethiopia.

Eritrea lies not only in Sudano-Sahelian region of Africa, which is predominantly characterized by arid and semi-arid climate and limited water resources [1], but also considered as one of the hottest countries on earth experiencing recurrent droughts. Despite the lack of adequate and reliable information on water resources, there are indications of presence of severe water shortages. The flows through the major rivers are highly seasonal with the exception of Setit River. Setit, the only perennial river that forms the border with Ethiopia, could not be fully utilized for major national development projects. Ground water has been the main water source for various uses supplemented by surface waters stored in dams and ponds. Climate ranges from hot and arid near the Red Sea to temperate sub-humid in the eastern highlands. Mean temperature varies between the agro-ecological zones, ranging from 18 °C in the highlands to 35 °C in the lowlands. Rainfall is torrential, of high intensity, short duration and is characterized by extreme spatio-temporal variability; less than 50 mm to over 1,000 mm falling mainly during the months of June to September. As a result of the topographically ragged nature of the highlands, thin soil formations and completely deforested terrains, most of the runoff turns into violent flash floods. Annual average precipitation is 384 mm [1]. Annual evapotranspiration rates range from 1,900 mm in the northern Red Sea coastal basin and plains, to 1,700 to 2,000 mm in the northern highlands and 8,000 mm in the Gash-Barka region [2].

Kozlov, D.V., Ghebrehiwot, A.A. Efficacy of digital elevation and Nash models in runoff forecast. Magazine of Civil Engineering. 2019. 87(3). Pp. 103–122. DOI: 10.18720/MCE.87.9.

Козлов Д.В., Гебрехиwот А.А. Эффективность цифровых моделей рельефа и моделей Нэша в прогнозировании стока // Инженерно-строительный журнал. 2019. № 3(87). С. 103–122. DOI: 10.18720/MCE.87.9



This open access article is licensed under CC BY 4.0 (<https://creativecommons.org/licenses/by/4.0/>)

Studies on the current situation of water resources in Eritrea [3] indicate that the government has made significant progress in the development of water resources through the construction of reservoirs, diversion structures and groundwater exploration for various water uses. Along with the artificial reservoirs with varying sizes that were constructed since independence, recently completed or still under construction such as Gheret, Kerkebet, Fanco, Ghergera, Gahtelay and Adi-Halo are some among others. Despite these promising endeavors, problems linked to the development and management of water resources have yet remained to be at the center stage of the government agenda due to manifold reasons. Critical analyses on the current status and use of water resources [3] reveal the absence of detailed studies on groundwater and surface water potentials. Moreover, modern knowledge about the water resources and hydrological information, which is crucial for the development of water management practices, are fragmented and in their initial stages of development.

Hydrometeorological observations on a regular basis began during the Italian colonial period. Nonetheless, when Eritrea gained independence, the water sector of the country was completely destroyed as a result of successive 30 years military action. Thus, the reasons for the poor quality of hydrometeorological information available today are not only successive breaks in the time series of observations, but also unreliability of the measurements. In recent years, an increasing trend in the establishment of hydrometeorological stations has been observed. However, their distribution and quality often do not meet the current national hydrometeorological observation network requirements. In addition, due to insufficient budget funding and poor coordination among the various executive authorities, the vast majority of existing stations lack proper operational scrutiny. This problem along with the complete absence of historical hydrological and meteorological data, in many cases, to date has been a major obstacle to the planning and development of projects for utilizing Eritrea's water resources [4, 5]. Under these circumstances along with structural and technical failures in the systems operation, it is difficult to achieve intended goals of water resources management projects. In one way or the other, these failures seem to be allied, among other things, to the use of improper assessment of river flow prediction approaches that do not consider the unique characteristics of the area under consideration. For example, the partial or complete failures of recently constructed diversion structures in the western lowlands of Eritrea justify this fact. At present, with the exception of limited and localized research developments [4, 5], there are no methods specifically developed for river basins characterized by the lack of hydrological observations. Hence, accurate and reliable approaches of river flow prediction for catchments under consideration can be either established or identified only on the basis of extensive applied research.

River flow modelling has become an important tool for planning and management of water management systems and facilities as well as the development of river forecasts and dissemination of warnings, for example, floods. The term "hydrological system modelling" includes time series analysis and stochastic modelling, which focuses on reproducing the statistical characteristics of the hydrological variable of a time series. To date, many models of river flow have been developed on such bases [6, 7]. Prediction of floods in hydrologically unexplored and poorly studied catchments, taking into account the unreliability of hydrometeorological information, has recently become one of the main directions of modern hydrological research. The transformation of the flood, during its passage through reservoirs and river beds can be determined by various methods, for example, hydrodynamic and hydrological.

According to the latter, in order to determine the arrival time and spreading of the flood wave formed as a result of heavy precipitation on the surface of the catchment, it is necessary to estimate the flow of water through the river system. For this purpose, a unit hydrograph (UH) theory [8] is usually constructed, which characterizes the time distribution of water flowing from the catchment [9]. In most practical problems, the generally accepted hydrological method of flood forecasting using UH theory cannot be implemented because it requires information about rainfall and runoff. Under such circumstances, different regionalized techniques are applied to develop synthetic unit hydrograph. Though it has various limitations, empirical equations require regional validity, which relate the salient hydrograph characteristics to basin characteristics. Moreover, it is strictly site specific, and cannot be considered as universal [10]. Kumar [11] pointed out limitations of regionalization: requires a large amount of rainfall-runoff data, inevitable heterogeneity of hydrological behavior of adjacent gauged catchments and periodical adjustment of model parameters that take care of unforeseen impacts of land use and climate change. The rational method based on the concept of hydrological zoning, according to Singh [7] is not only applicable for solving problems of water related design but also fails to generate complete information about river flow.

Dooge [12] developed a more complete conceptual model for the calculation of UH and showed that for rivers where there are no available hydrological observations, it is advisable to establish generalized UH. But, since the equation of UH was not easily solvable for complex problems, various simplifications were proposed. For example, the procedure for constructing a UH developed by Snyder [13] is based on the analysis of a large number of basins and single hydrographs in order to obtain a relationship between the shape of a UH and the physical and geographical characteristics of the catchment. In Snyder's approach, the coefficients of the equation associated with the physical and geographical characteristics of the basin vary significantly sometimes over a range of 10 times [14] leading to inaccurate estimates of floods. According to Pilgrim [14],

due to the empirical nature of Snyder's approach, its application should be limited to the region for which these coefficients were obtained.

To overcome the difficulties associated to the dependence of UH on the effective rainfall duration, instantaneous unit hydrograph (IUH) [7] that considers vanishingly small duration has been introduced since long time back. The IUH is the unit impulse response or characteristic response of a catchment. It is widely applied because it can reflect the characteristic of valley flow concentration [15] and much more important information about the basin characteristics can also be extracted. Numerous hydrological conceptual models have been proposed to develop IUH. These models consider a catchment as a system that converts the input effective rainfall into a flood. For example, a conceptual cascade of linear reservoirs was proposed [12, 16, 17] to simulate the process of transformation of precipitation into runoff. Nash [18] developed a general theory of the IUH which is represented by a linear scheme of river channels and reservoirs. However, the limitations in the application of these models for ungauged catchments are proven [19] due to the nonlinear nature of the relationship between precipitation and runoff. Moreover, conceptual models contain large numbers of parameters that cannot be related to physical watershed characteristics [4, 20]: hence, they must be estimated by calibration using observed data.

Under such circumstances, the use of geomorphologic instantaneous unit hydrograph (GIUH) approach [21], which is based upon the widespread use of laws of stream orders proposed by Horton [22] and later modified by Strahler [23], is required. Rodriguez-Iturbe and Valdes [21] developed a physical methodology for the derivation of IUH using the empirical laws of geomorphology and climate characteristics. Specifically, the GIUH approach has two specific advantages: no requirement of historical flow records and ability to develop IUH using only topographic maps or remote sensing data that can be done using freely available shuttle radar topography mission (SRTM) data in geographical information system (GIS) environment. Gupta and others [24] related the parameters (peak and time peak) of IUH with geomorphologic characteristics of the catchment with a varying dynamic velocity parameter. Difficulties arise in the estimation of dynamic velocity parameter that has different values for each flood event: hence, it requires intermittent evaluation. Later, it was rationalized as a function of the effective rainfall intensity and duration to produce a concept of GIUH [25]. In this concept, the governing equations become a function of the mean effective rainfall intensity, Manning's roughness coefficient, average width and slope of the highest order stream. Rosso [26] related the Horton's order ratios [22] to the parameters of Nash model through power regression. Yen and Lee [19, 27] developed a geomorphology and kinematic-wave and stream order laws based hydrograph derivation. As such, GIUH became more powerful technique than the parametric Clark model [16] and Nash model [18]. To avoid the limitation of parameter estimation due to scanty hydrometeorological data in ungauged catchments, coupling of models has become a common practice. The GIUH from the watershed geomorphologic characteristics was related to the Nash model parameters [28] and Clark model [11]. Recently, a new method to estimate the Nash model parameters on the basis of the concept of geomorphologic dispersion stemming from spatial heterogeneity of flow paths within a catchment [29] has been formulated. The reliability and accuracy of Nash model based GIUH as compared to other approaches are shown in the works of [6, 11, 28, 30]. Nonetheless, Guzha and others [31] argue that coupling of two or more models can result in inconsistencies because the individual models may describe the same processes in different ways. However, the recent works on the applicability of the GIUH-Nash based model for the derivation of UH [4] show the adequacy of the GIUH-Nash model for the derivation of UH suggesting for further research aiming at assessing the impact of the resolution and source of digital elevation model (DEM) on the direct runoff predictions. On the basis of this suggestion, this paper will investigate the efficacy of DEM and quantum geographic information system (QGIS)-based computational algorithms for obtaining river flow information based on the GIUH-Nash model.

A DEM is defined as any digital representation of a continuous change in elevation in space that can be derived from topographic maps and satellite imagery. It is the most important source of data on topography and catchment characteristics, which are widely used in numerous hydrological studies. Nonetheless, DEM data are often used in hydrological studies without quantifying the effects of errors that constitute uncertainty [32]. Areas related to the uncertainty of the DEM that affect its use for hydrological applications include: the DEM error, topographic parameters often derived from the DEM and related algorithms used to derive these parameters, the influence of the scale of the elevation matrix as determined by the resolution of the grid cell, the interpolation of the elevation matrix and the modification of the terrain surface used to create hydrologically viable elevation matrix surfaces. Each of these areas contributes to the uncertainty of the DEM and can potentially influence the results of hydrological models with distributed parameters that rely on the DEM to obtain model inputs. In modern hydrology, a significant amount of research has been carried out [32] to eliminate the uncertainty associated with errors in DEM and to use appropriate solutions to improve the input parameters of models. For example, Lawrence Hawker and others [9] have identified three approaches to correcting the DEM error: editing the DEM, new elevation matrices created using advanced sensing technologies and stochastic modeling of the elevation matrix.

In the works of Weschler [32, 33], the inadequate level of attention paid by users of DEM to the question of uncertainty of DEM and its influence on various topographic parameters often used in hydrological studies is presented. Moreover, not only the accuracy of DEM depends on resolution but also the quality of the primary

source in which the DEM is generated significantly affects the topographical parameters of the DEM [34]. Size and accuracy of DEM resolution has a direct impact on the forecast of hydrological information on models, for example, TOPMODEL [35] and SWAT [36, 37]. However, when it comes to the generation of topographical parameters from DEM, it appears that the higher resolution of DEM is not necessarily better than the lower resolution [37]. On the other hand, the efficiency of the rainfall-runoff models that depend on the river network characteristics are impacted by the resolution of the selected DEM and threshold values [38]. Therefore, understanding the implications of DEM and GIS-based algorithms on various parameters should be the first step in hydrological modelling.

Keeping view of aforesaid facts and considering unavailability of literatures that indicate how the DEM and algorithm selection affect runoff prediction based on GIUH-Nash model, the present study was intended to solve mainly the problem of quantitative assessment of runoff from ungauged catchments in the absence or insufficiency of hydrological information within the framework of the following specific tasks: (1) evaluation of the effectiveness of DEM in predicting direct surface runoff using the GIUH-Nash model, and (2) evaluation of the impact of stream network formation algorithms on the prediction of direct surface runoff using the GIUH-Nash model. To this end, various methods were employed and are explained in the ensuing section.

2. Methods

The subject of this study is to assess the effectiveness of digital elevation models and GIUH-Nash models in predicting surface runoff for the unexplored Mereb-Gash river Debarwa catchment in Eritrea.

This research is an applied research that intends to find a solution for some of the pressing practical problems in water resources development and management projects in Eritrea. Thus, the approach employed is primarily based on the widely known conceptual, linear, time-invariant Nash-model coupled with the geomorphologic, physical and geographical characteristics derived from open-source DEMs. QGIS software is intensively used to process, analyze and map the DEMs-based data. Apparently, GIUH-Nash model is purely an analytical method whose parameters can be determined explicitly with the exception of scale parameter, n which is determined implicitly. The computed outputs of the model are calibrated using five recorded storm events. The details of the adopted methods are presented in the ensuing sub-sections.

2.1. Study area

The object of the study is the Debarwa catchment area with its outlet near the town of Debarwa, located in the southern region of Eritrea. Its outlet is specifically located at 15°05'49" N latitude and 38°50'11" E longitude about 29 km south of the capital in the eastern part of the Mereb-Gash river basin (Figure 1). The drainage area is estimated to be 200 km² with its elevation varying between 1,905–2,550 m above mean sea level. The watershed comprises hilly and dissected mountains mainly covered with open and sparse shrubs and mild slope agricultural lands (Figure 2). As per the information obtained from the 30 m resolution SRTM-based DEM, average basin slope is equal to 13.325 %. The main channel is 37 km long with a longitudinal slope of 1.16 %. Drainage density and channel segment frequency are 0.64 km/km² and 0.21 streams per km², respectively. According to the agro-ecological classification of Eritrea, the Debarwa catchment lies in moist highlands zone where temperature varies from 0 °C to 32 °C and an average annual rainfall of 547 mm. Climate in the catchment can be characterized as moderate with December-January being the coldest and March-April the hottest. Maximum precipitation occurs in the summer season, specifically in the months of July and August with a monthly mean rainfall of 185 mm and 175 mm, respectively.

2.2. Geomorphologic database

The physical characteristics of stream channels of a drainage basin can provide helpful information through the likely effects of the variation of hydraulic radius and roughness on average flow velocities [14]. The success of the GIUH-based model also completely relies upon the quality of stream channels formation. In this study, four frequently used open-source DEMs were considered for the extraction of geomorphological database of the catchment with the help of the freely available QGIS software. They are based on geo data of several global elevation matrices: level-1 with a resolution of 90 m (3-arc seconds) and level-2 data with a resolution of 30 m (1-arc second). Specifically, the DEMs include two shuttle radar topographic mission (SRTM 90 and SRTM 30), 30-m resolution data from the advanced space thermal emission and reflection radiometer (ASTER 30) and 30m resolution data from advanced land observing satellite - JAXA's Global ALOS 3D (ALOS 30). The georeferenced and QGIS compatible file format (GeoTiff) files of the four DEM-sources were imported to QGIS. Accordingly, the geomorphological database of the study area was established using two of the best known open-source QGIS packages: geographic resources analysis support system (GRASS) and system for automated geoscientific analyses (SAGA).

The geospatial data analysis library (GDAL) has been used to handle the raster geographic data formats of DEM. As such, multi-layered raster was created in the original virtual directory so as to delineate the catchment area. Using the `gdalbuildvrt` utility of the GDAL library, a virtual mosaic of the dataset (`vrt`) of the catchment was established from all GeoTiff input files. The mosaic from the original rasters meets the

following conditions: all images must be in the same coordinate system and have the same number of bands, but the resolution may be different and the rasters may overlap. The raster file of the mosaiced virtual dataset was reprojected by using an algorithm derived from the GDAL warp utility. The sinks in the output file were filled using the fill sinks function from SAGA to get filled DEM and flow directions. As such, Strahler order raster and channel network in vector form were produced from the channel network and drainage basin algorithm in SAGA. The raster of the catchment was delineated from the filled DEM input using the watershed basin analysis program in SAGA and appropriate value of the minimum size of exterior watershed basin criteria. The co-ordinates of the outlet for the watershed under consideration were identified using the co-ordinate capture plugin tool. Using the drainage direction as input in the watershed creation program in GRASS and the outlet co-ordinates, the required catchment was extracted. After converting the watershed in raster file into vector format, the GDAL extraction function was then used to clip raster DEM and area of interest is extracted. On top of this, the channels file was also clipped to the area of interest using the clip function in vector overlay tools. From these processes four DEM versions were obtained for the study area.

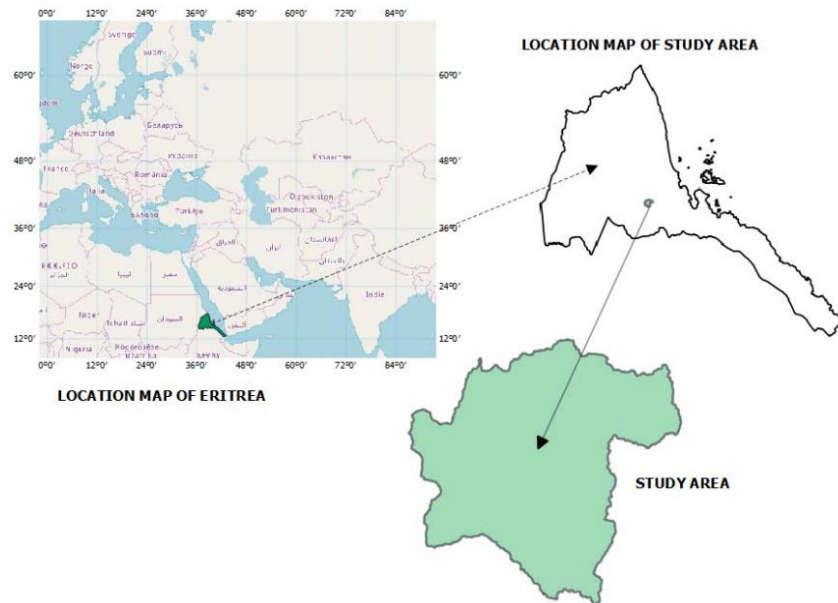


Figure 1. Location map of Eritrea and study area [4].

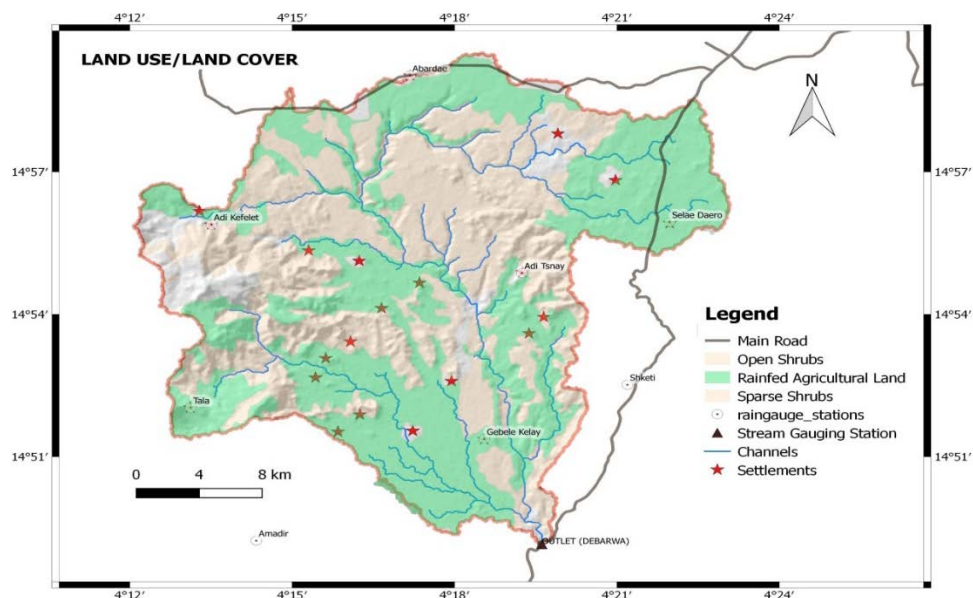


Figure 2. Land use/land cover map of Debarwa catchment [4].

To study the implication of algorithms on virtual channel network creation and in the geomorphologic database preparation, watershed basin analysis program from GRASS and channel network and drainage basins from SAGA were used. Apparently, the noticeable difference among these two algorithms is the threshold value assignment. The former uses number of cells and the later uses stream orders. In the GRASS-algorithm, the values of minimum size of exterior watershed basin were intuitively chosen to be 1,500 cells for SRTM 30, ASTER 30 and ALOS 30 and 166 cells for SRTM 90, respectively. All of them produce a catchment with the same number of stream orders, the highest being fourth order (Figure 3). In the SAGA-

algorithm, threshold values of 6 and 4 for the 30 m and 90 m resolutions are applied, respectively (Figure 4). The overall patterns of the channel networks and the number of stream orders from both algorithms are relatively similar. Nevertheless, discrepancy in the lengths of the highest ordered channels are easily noticeable in the outputs from the 30 m resolution DEMs. The algorithm from GRASS produce longer fourth order channels (18436 m) than that of SAGA (1423 m). On the contrary, the 90 m resolutions DEMs generate nearly the same lengths of fourth ordered channels; 18621 m and 16484 m by GRASS and SAGA, respectively. To what extent would these and other unforeseen discrepancies affect the performance of the GIUH-Nash model-based runoff predictions?

To address the above question, four DEM-scenarios were considered for each algorithm obtained using the aforementioned procedures. In each case, stream lengths, elevations at the stream junctions, stream numbers and their orders and other attributes were processed and stored. The most tedious and time consuming part of the work was the on-screen digitization of the areas corresponding to the i^{th} stream order of the eight scenarios. Eventually, the bifurcation ratios (R_B), length ratios (R_L) and area ratios (R_A) are calculated according to Horton's laws based on the following relationships: law of stream numbers $R_B = N_\omega / N_{\omega+1}$, law of stream lengths $R_L = \bar{L}_\omega / \bar{L}_{\omega-1}$ and law of stream areas $R_A = \bar{A}_\omega / \bar{A}_{\omega-1}$; where N_ω is the number of streams, \bar{L}_ω is the mean length of streams, and \bar{A}_ω - the mean area of the basins of order, ω . The ratios in nature are normally between 3 and 5 for R_B , between 1.5 and 3.5 for R_L , and between 3 and 6 for R_A , respectively [21].

The geomorphological parameters namely R_B , R_L and R_A are computed graphically by plotting stream orders versus logarithm transformed stream numbers (N_s), mean stream length (L_m) and mean stream areas (A_m), respectively so as to have a linear relationship among the variables. The actual values of the ratios (Figure 5) are obtained from the slopes of the best fit lines corresponding to bifurcation, length and area ratios, respectively. Some of the GRASS-based and SAGA-based geomorphological parameters for the study area are presented in Table 1 and Table 2, respectively.

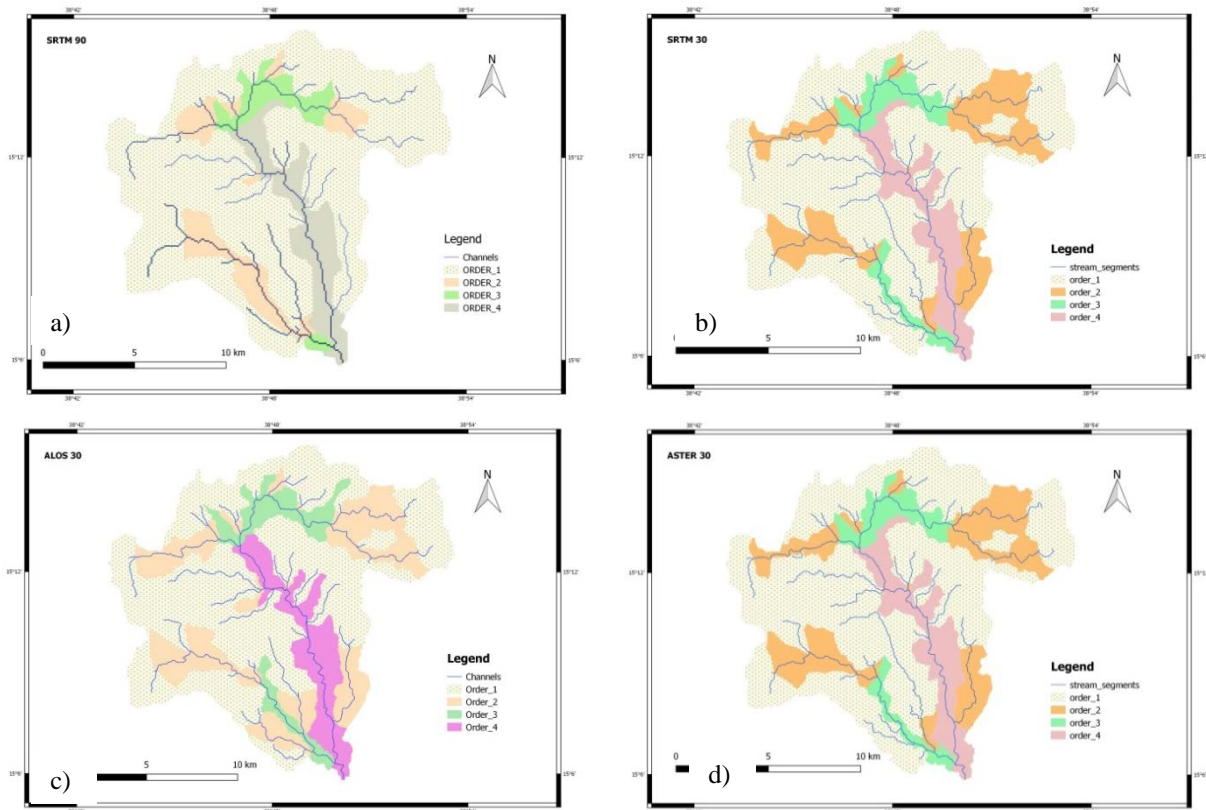


**Figure 3. Channel systems and stream areas from GRASS [4]:
a) SRTM 90 and b) SRTM 30 c) ALOS 30 and d) ASTER 30.**

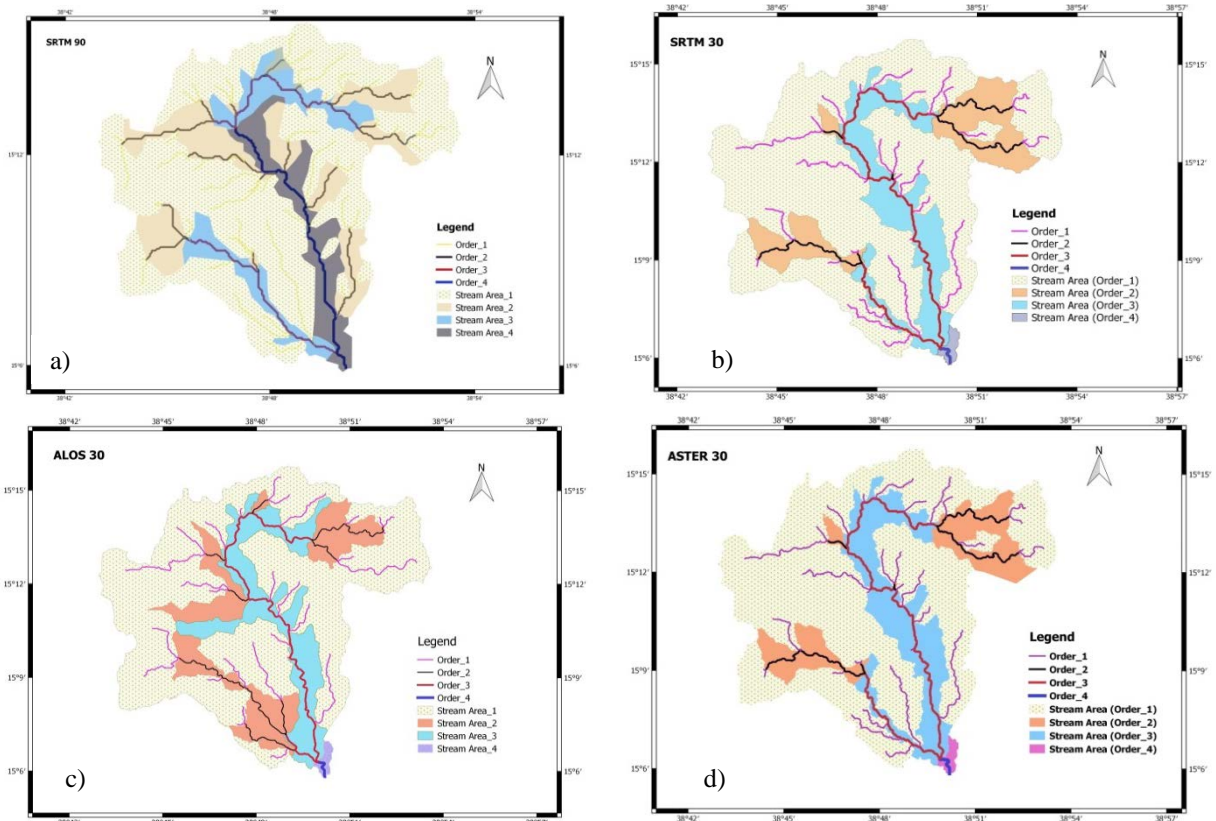


Figure 4. Channel systems and stream areas from SAGA [4]: a) SRTM 90 and b) SRTM 30 c) ALOS 30 and d) ASTER 30.

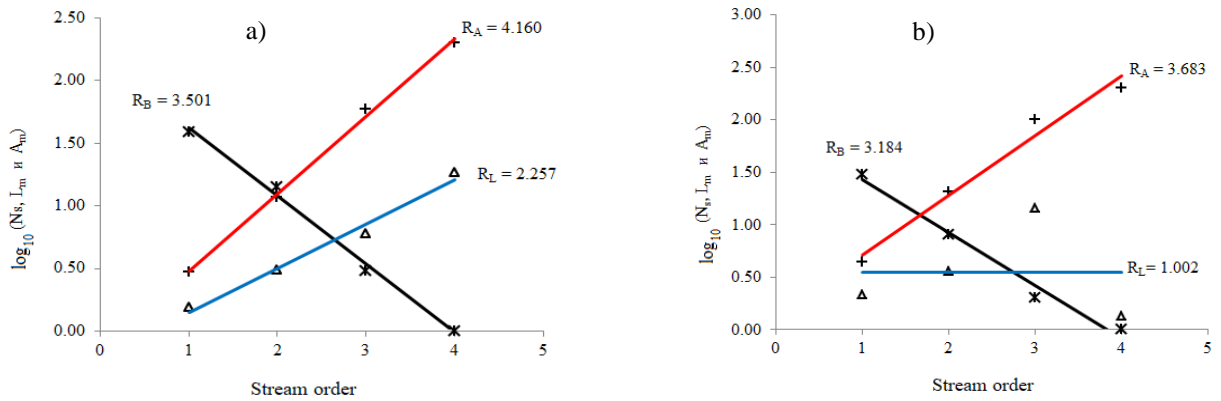


Figure 5. Examples of Horton's laws based ratios from ALOS 30: a) GRASS and b) SAGA.

Table 1. GRASS-based geomorphologic characteristics of Debarwa Catchment.

| DEM | Stream Order (ω) | No of streams (N_ω) | stream length L (km) | mean stream length \bar{L}_ω (km) | mean stream area \bar{A}_ω (km ²) | R_B | R_L | R_A |
|----------|---------------------------|------------------------------|------------------------|--|--|-------|-------|-------|
| ALOS 30 | 1 | 39 | 59.856 | 1.535 | 2.979 | 3.501 | 2.257 | 4.160 |
| | 2 | 14 | 43.303 | 3.093 | 11.670 | | | |
| | 3 | 3 | 17.987 | 5.996 | 59.596 | | | |
| | 4 | 1 | 18.572 | 18.572 | 200.262 | | | |
| ASTER 30 | 1 | 40 | 68.252 | 1.706 | 3.104 | 3.474 | 2.183 | 4.039 |
| | 2 | 12 | 37.765 | 3.147 | 13.514 | | | |
| | 3 | 3 | 18.571 | 6.190 | 58.851 | | | |
| | 4 | 1 | 18.368 | 18.368 | 199.453 | | | |
| SRTM 30 | 1 | 40 | 68.252 | 1.706 | 3.104 | 3.474 | 2.183 | 4.039 |
| | 2 | 12 | 37.765 | 3.147 | 13.514 | | | |
| | 3 | 3 | 18.571 | 6.190 | 58.851 | | | |
| | 4 | 1 | 18.368 | 18.368 | 199.453 | | | |
| SRTM 90 | 1 | 34 | 67.141 | 1.975 | 4.088 | 3.383 | 2.113 | 3.794 |
| | 2 | 10 | 24.412 | 2.441 | 16.551 | | | |
| | 3 | 2 | 10.299 | 5.149 | 88.384 | | | |
| | 4 | 1 | 18.621 | 18.621 | 199.179 | | | |

Table 2. SAGA-based geomorphologic characteristics of Debarwa catchment.

| DEM | Stream Order (ω) | No of streams (N_ω) | stream length L (km) | mean stream length \bar{L}_ω (km) | mean stream area \bar{A}_ω (km ²) | R_B | R_L | R_A |
|----------|---------------------------|------------------------------|------------------------|--|--|-------|-------|-------|
| ALOS 30 | 1 | 30 | 64.140 | 2.138 | 4.382 | 3.184 | 1.002 | 3.683 |
| | 2 | 8 | 29.108 | 3.639 | 20.690 | | | |
| | 3 | 2 | 29.008 | 14.504 | 99.467 | | | |
| | 4 | 1 | 1.357 | 1.357 | 200.232 | | | |
| ASTER 30 | 1 | 32 | 66.885 | 2.090 | 4.281 | 3.206 | 0.945 | 3.662 |
| | 2 | 7 | 22.919 | 3.274 | 23.394 | | | |
| | 3 | 2 | 34.158 | 17.079 | 99.401 | | | |
| | 4 | 1 | 1.456 | 1.456 | 200.066 | | | |
| SRTM 30 | 1 | 32 | 66.868 | 2.090 | 4.215 | 3.157 | 1.042 | 3.597 |
| | 2 | 6 | 22.919 | 3.820 | 26.928 | | | |
| | 3 | 2 | 34.158 | 17.079 | 97.340 | | | |
| | 4 | 1 | 1.456 | 1.456 | 196.006 | | | |
| SRTM 90 | 1 | 63 | 85.042 | 1.350 | 1.897 | 4.121 | 2.378 | 4.882 |
| | 2 | 17 | 41.936 | 2.467 | 9.399 | | | |
| | 3 | 3 | 23.558 | 7.853 | 60.626 | | | |
| | 4 | 1 | 16.484 | 16.484 | 201.120 | | | |

2.3. Development of the GIUH-Nash Model

2.3.1. Nash model

One of well-known and widely used models is Nash cascade [18] which can be visualized as a sequence of n linear reservoirs in series, each of which has a time lag of K , during which individual precipitation is instantly superimposed on the upper reservoir. A linear reservoir is a reservoir for which there is a linear relationship between the storage of each tank and the output. An input of a unit of excess rainfall over the catchment is applied instantaneously to the first reservoir. The routed outflow from the first reservoir becomes the input to the second reservoir in series and the second reservoir output becomes the input to the third, and so on. Output from the last n^{th} reservoir is the output from the system representing an IUH for the catchment. The resulting mathematical form for the unit hydrograph $q(t)$ is equivalent to the gamma distribution:

$$q(t) = \frac{1}{\Gamma(n)} \frac{1}{K} \left(\frac{t}{K}\right)^{n-1} e^{-t/K}, \quad (1)$$

where $q(t)$ is the IUH of the Nash model;

$\Gamma(n)$ is the Gamma function;

K is the storage coefficient in h .

The parameters, n and K , can be determined by a number of ways; the most widely used being the method of moments. Mathematically, n may take fractional values [6] so as to give a wider range of shapes in fitting the observed data. Direct determination of the above parameters requires reliable historical records of rainfall-runoff. In the absence of historical rainfall-runoff data, they are determined as described below.

2.3.2. GIUH-Nash model

According to Beven [6], GIUH method is still widely used as a tool for predicting flood discharges in ungauged catchments: it has the advantage of using it in situations where there is insufficient amount of input information and is simple for practical application. The estimation of the GIUH for a given catchment allows the user to use this hydrograph for any case of precipitation in the catchment and therefore to assess its response.

The relationship between the peak discharge q_p and time peak t_p of the IUH as a function of the geomorphologic characteristics of the catchment [21] is given as follows,

$$q_p = 1.31 R_L^{0.43} (V / L_\Omega) \quad (2)$$

and

$$t_p = 0.44 \left(\frac{L_\Omega}{V}\right) \left(\frac{R_B}{R_A}\right)^{0.55} R_L^{-0.38}, \quad (3)$$

where Ω is stream order of the catchment;

L_{Ω} is length of the highest order stream (km);

V is dynamic velocity parameter (ms^{-1}). The parameters q_p and t_p have units (h^{-1}) and (h), respectively. Multiplication of equations (2) and (3) that have units of time gives a non-dimensional term which is independent of the dynamic velocity and storm characteristics. It is purely a function of the geomorphologic characteristics:

$$q_p \times t_p = 0.5764 \left(\frac{R_B}{R_A} \right) 0.55 R_L^{0.05}, \quad (4)$$

The first derivative of (1) gives the time to peak as follows,

$$t_p = (n-1) \times K. \quad (5)$$

Substituting this value for t_p in (1), the peak discharge q_p of the IUH is obtained as,

$$q_p = \frac{(n-1)^{n-1}}{K \times \Gamma(n)} \times e^{-(n-1)}. \quad (6)$$

The product of (5) and (6) gives a function of the Nash-parameter, n . Thus,

$$q_p \times t_p = \frac{(n-1)^n}{\Gamma(n)} \times e^{-(n-1)}. \quad (7)$$

Equating (4) and (7), the following relationship is arrived at:

$$\frac{(n-1)^n}{\Gamma(n)} \times e^{-(n-1)} = 0.5764 \left(\frac{R_B}{R_A} \right)^{0.55} R_L^{0.05}. \quad (8)$$

The value of n in equation (8) can be solved by Newton-Rapson iteration or Matlab optimization tool. Rearranging (5) and substituting the right hand side of (3) for t_p , the value of K could be solved as,

$$K = \frac{0.44}{n-1} \times \left(\frac{L_{\Omega}}{V} \right) \left(\frac{R_B}{R_A} \right)^{0.55} R_L^{-0.38}. \quad (9)$$

The dynamic velocity proposed is the velocity corresponding to the peak runoff for a given rainfall-runoff event in the catchment. This velocity can be obtained with the help of Manning's equation [4, 10, 11].

$$V = \frac{1}{n_m} R^{2/3} S_m^{1/2}, \quad (10)$$

where n_m is Manning's roughness coefficient;

R is hydraulic radius;

S_m is slope of the main channel.

The value of the roughness coefficient is influenced by hydraulic flow elements (depth, slope), including those associated with changes in cross-section and river bed. For example, the values of n_m may decrease with increasing depth or flow to the level of water discharge to floodplain, when floods remain confined within the channel banks [14], which has been the case of the study area. It should be noted that in the Debarwa catchment, a permanent hydrometric gauging station is installed along one of the concrete walls of the Debarwa bridge with a rocky cobbles river bed. Given these boundary conditions and performing trial and error to obtain optimal prediction of the desired hydrograph, n_m was taken to be 0.022. S_m is computed using the «85-10» slope factor method [7].

Since Manning's coefficient n_m greatly affects the dynamic velocity V and time lag K in the GIUH-Nash model, its actual value must be studied before applying the model for hydrological modeling.

2.3.3. Direct surface runoff computation

The ultimate objective of GIUH development is to derive a UH of required duration which in turn can be used for computation of direct surface runoff. Thus, equation (11) is applied for this purpose. Pilgrim

recommends the use of a period longer than a quarter of the UH time peak may result in large errors, especially at the hydrograph peak. Accordingly, since the time peak in most of the derived UHs from the observed stream flows is one hour, 0.25 hour UH duration is used. The relationship between IUH [$u(t)$] and D-hour UH [$U(D, t)$], both of the same unit depth, are related by the formula:

$$U(D, t) = \frac{\int_0^t u(t) dt}{D}, \quad (11)$$

where D is the duration of the UH.

Eventually, the direct runoff hydrograph is estimated by convoluting the excess rainfall hyetograph with the UH obtained from equation (11) for all storm events corresponding to each DEM-scenario and algorithm. The predicted direct runoffs were compared with five single peaked storm events so as to evaluate the GIUH-Nash model. Various objective fit functions and statistical indices are also used for this purpose as presented in the ensuing sub-section.

2.3.4. Model evaluation

Since all models and their parameters are approximations to reality, comparing the computed results and observed data is a must in hydrologic modelling. To this end, several model evaluation techniques are employed for judging the fit of calculated to observed hydrograph. In this study, the differences between peak magnitudes, a measure of overall fit such as the sum of absolute values or squares of the differences of individual ordinates, or differences between lags or other time measures were used. Moreover, visual inspection of the shape and major characteristics of the hydrographs (time peak, peak discharge, and time base) for different storm events were applied. The standard regression and error indices used in the study are briefly explained in the ensuing paragraphs.

Nash-Sutcliffe efficiency (NSE): The efficiency of a hydrological model is measured by the NSE, which determines the relative magnitude of the residual variance compared to the measured data variance [39]. It indicates how well the plot of observed versus simulated data fits the 1:1 line given by:

$$NSE = 1 - \frac{\sum_{t=1}^N [Q_o(t) - Q_p(t)]^2}{\sum_{t=1}^N [Q_o(t) - \bar{Q}_o]^2}. \quad (12)$$

Nash-Sutcliffe efficiency can range from $-\infty$ to 1. An efficiency of 1 ($NSE = 1$) corresponds to a perfect match of modelled discharge to the observed data. An efficiency of 0 ($NSE = 0$) indicates that the model predictions are as accurate as the mean of the observed data, whereas an efficiency less than zero ($NSE < 0$) occurs when the observed mean is a better predictor than the model or, in other words, when the residual variance (described by the numerator in the expression above), is larger than the data variance (described by the denominator). Essentially, the closer the model efficiency is to 1, the more accurate the model is.

Special correlation coefficient (SC): a goodness of fit between observed and predicted is also given by:

$$SC = \sqrt{\frac{2 \sum_{t=1}^N Q_o(t) Q_p(t) - \sum_{t=1}^N [Q_p(t)]^2}{\sum_{t=1}^N [Q_o(t)]^2}}. \quad (13)$$

Mean absolute error (MAE) and root mean square error (RMSE): These indices allow us to estimate how the values of the sets of observed and predicted values may differ from the average, which helps in the analysis of the results. The RMSE value is important for determining the plausibility of the phenomenon under study in comparison with the predicted value of the model: if the average value of measurements is very different from the predicted values of the model (a large value of the standard deviation), then the values obtained or the method of obtaining them should be rechecked. The value 0 indicates a perfect match between the model and nature. The MAE and RMSE values can be calculated from equations (14) and (15), respectively:

$$MAE = \frac{\sum_{t=1}^N |Q_o(t) - Q_p(t)|}{N}, \quad (14)$$

$$RMSE = \sqrt{\frac{\sum_{t=1}^N [Q_o(t) - Q_p(t)]^2}{N}}, \quad (15)$$

where $Q_o(t)$ and $Q_p(t)$ are observed and predicted direct runoff rates at time t , respectively,

N is total number of ordinates of direct runoff hydrograph (DRH).

Indices of simulation of single-event allow us estimation of the accuracy of predicted hydrograph ordinates. For this purpose, we used three methods: error of the direct runoff volume (EV), the relative error at the peak (REP) and the uncertainty of the time occurrence of peak (ETP) [11].

$$EV = \frac{V_o - V_p}{V_o} \times 100, \quad (16)$$

$$REP = \frac{Q_o - Q_p}{Q_o} \times 100, \quad (17)$$

$$ETP = T_p - T_o, \quad (18)$$

where V_o and V_p are observed and predicted runoff volumes;

Q_o and Q_p are observed and predicted peak runoff rates;

T_o and T_p are time peak of observed and predicted runoffs, respectively.

3. Results and Discussions

Prior to the application of the selected model, intensive analyses were carried out on various physical and geographical parameters so as to observe the discrepancies and uncertainties among the DEMs and, of course, to determine the parameters to be used in the model. Details of these parameters obtained from four DEMs are presented in Table 3. A noticeable discrepancies and uncertainties among them could be seen in some of these parameters. For example, the basin area obtained from ALOS 30, ASTER 30 and SRTM 90 are larger (~200 km²) than SRTM 30 (~196 km²) whereas the 30 m resolution DEMs produced higher basin slope (~13.4 %) as compared to the 90 m DEM (8.662 %). The vast majority of the physical and geographical parameters obtained from lower resolutions are higher than DEMs of higher resolution.

Table 3. DEM-wise physiographic parameters of Debarwa catchment.

| Physiographic parameter | DEM-Scenarios | | | |
|---|---------------|----------|----------|----------|
| | ALOS 30 | ASTER 30 | SRTM 30 | SRTM 90 |
| Average basin slope (%) | 13.382 | 13.872 | 13.325 | 8.662 |
| Basin area (km ²) | 200.232 | 200.066 | 196.006 | 201.120 |
| Basin perimeter (km) | 101.494 | 109.675 | 103.737 | 98.472 |
| Basin relief (km) | 0.673 | 0.617 | 0.643 | 0.639 |
| Channel segment frequency (no. /km ²) | 0.205 | 0.210 | 0.209 | 0.418 |
| Circularity ratio | 0.244 | 0.209 | 0.229 | 0.261 |
| Constant of channel maintenance (km ² /km) | 1.620 | 1.595 | 1.563 | 1.204 |
| Drainage density (km/km ²) | 0.617 | 0.627 | 0.640 | 0.830 |
| Elongation ratio | 0.851 | 0.851 | 0.842 | 0.853 |
| Fineness ratio | 1.218 | 1.144 | 1.209 | 1.696 |
| Form factor | 0.569 | 0.569 | 0.557 | 0.572 |
| Main channel length (km) | 36.682 | 36.891 | 36.891 | 33.697 |
| Main channel slope (%) | 1.083 | 1.130 | 1.162 | 1.214 |
| Maximum basin length (km) | 18.757 | 18.757 | 18.757 | 18.757 |
| Maximum elevation (m) | 2575.694 | 2527.694 | 2549.139 | 2555.151 |
| Minimum elevation (m) | 1902.833 | 1902.833 | 1905.936 | 1916.185 |
| Relief ratio | 0.036 | 0.033 | 0.034 | 0.034 |
| Ruggedness number | 0.415 | 0.387 | 0.412 | 0.531 |
| Shape factor | 2.297 | 2.311 | 1.961 | 2.106 |
| Unity shape factor | 1.326 | 1.326 | 1.340 | 2.376 |

To further verify the uncertainties and discrepancies among the DEMs, longitudinal and transversal elevation profiles of the main channel length (MCL) were checked. For example, longitudinal profiles of DEMs taken near 10 % of MCL (Figure 6) and transversal profiles of DEMs taken at 85 % of MCL (Figure 7) are presented below. As pointed out in the methods section, 85 % and 10 % of MCL measured from the outlet are used for the determination of S_m . Graphical results of these profiles indicate absolute overlapping of SRTM 30 and ASTER 30 DEMs whereas significant elevation differences could be clearly observed among SRTM 90, ALOS 30 and SRTM 30–ASTER 30. Besides, in most cases, the elevations of SRTM 90 are significantly higher than other DEMs. Even though statistical verification of these variations could not be done on account of lack of ground control points, these elevation profiles and values of physiographic parameters comply with the conclusions of Wechsler [32].

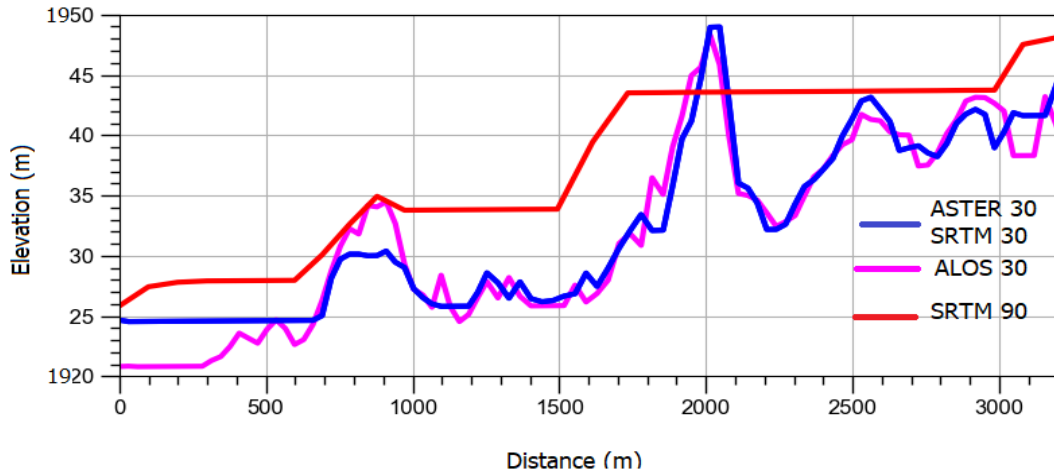


Figure 6. Longitudinal profiles of DEMs at 10 % of the main channel length (MCL).

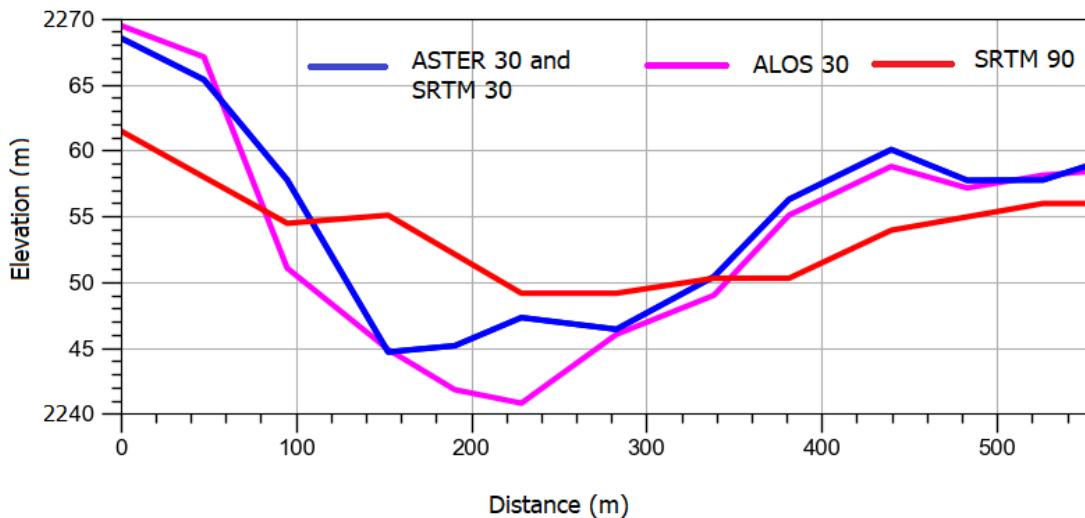


Figure 7. Transversal profiles of DEMs at 85 % the main channel length (MCL).

The Nash model parameters are calculated from equations (8) and (9), respectively. Nash parameters, peak runoff and time peak for various storm events obtained from the selected algorithms are presented in Table 5 and Table 6. The results of the calculations for the four DEM-scenarios indicate that values of n and K obtained from GRASS-based stream networks are higher, in most cases, than those of SAGA-based. The reason behind this disparity and their implications on the performance of the model was investigated and is discussed in the ensuing paragraphs.

Table 4. GRASS-based dynamic velocity and scale parameter.

| Storm event | ALOS 30 | | ASTER 30 | | SRTM 30 | | SRTM 90 | |
|-----------------|-----------|---------|-----------|---------|-----------|---------|-----------|---------|
| | V , m/s | K , h | V , m/s | K , h | V , m/s | K , h | V , m/s | K , h |
| July 17, 2006 | 6.220 | 0.431 | 6.354 | 0.420 | 6.445 | 0.414 | 6.587 | 0.410 |
| August 02, 2006 | 6.617 | 0.405 | 6.759 | 0.395 | 6.855 | 0.389 | 7.007 | 0.386 |
| August 04, 2006 | 6.455 | 0.415 | 6.593 | 0.405 | 6.687 | 0.399 | 6.835 | 0.395 |
| August 16, 2006 | 5.531 | 0.485 | 5.650 | 0.473 | 5.731 | 0.466 | 5.857 | 0.461 |
| August 22, 2006 | 8.043 | 0.333 | 8.215 | 0.325 | 8.333 | 0.320 | 8.517 | 0.317 |

Table 5. GRASS-based values of Nash parameters, peak runoff and time peak.

| Storm event | DEM | Nash parameters | | Peak runoff | | | Time peak | | |
|-----------------|----------|-----------------|---------|---------------------------|---------------------------|-------------------------------|-----------|-----------|---------------|
| | | n | K , h | Q_o , m ³ /s | Q_p , m ³ /s | Q_{avg} , m ³ /s | T_o , h | T_p , h | T_{avg} , h |
| July 17, 2006 | ALOS 30 | 3.035 | 0.431 | 61.921 | 61.299 | 62.137 | 0.50 | 1.25 | 1.25 |
| | ASTER 30 | 3.071 | 0.420 | | 62.039 | | | 1.25 | |
| | SRTM 30 | 3.071 | 0.414 | | 62.827 | | | 1.25 | |
| | SRTM 90 | 3.142 | 0.410 | | 62.382 | | | 1.25 | |
| August 02, 2006 | ALOS 30 | 3.035 | 0.405 | 66.860 | 71.627 | 72.360 | 1.00 | 1.25 | 1.25 |
| | ASTER 30 | 3.071 | 0.395 | | 72.245 | | | 1.25 | |
| | SRTM 30 | 3.071 | 0.389 | | 73.029 | | | 1.00 | |
| | SRTM 90 | 3.142 | 0.386 | | 72.737 | | | 1.25 | |
| August 04, 2006 | ALOS 30 | 3.035 | 0.415 | 73.301 | 67.837 | 68.657 | 1.00 | 1.25 | 1.00 |
| | ASTER 30 | 3.071 | 0.405 | | 68.573 | | | 1.00 | |
| | SRTM 30 | 3.071 | 0.399 | | 69.710 | | | 1.00 | |
| | SRTM 90 | 3.142 | 0.395 | | 68.968 | | | 1.25 | |
| August 16, 2006 | ALOS 30 | 3.035 | 0.485 | 44.585 | 56.801 | 56.250 | 1.00 | 1.25 | 1.00 |
| | ASTER 30 | 3.071 | 0.473 | | 53.105 | | | 1.00 | |
| | SRTM 30 | 3.071 | 0.466 | | 58.078 | | | 1.00 | |
| | SRTM 90 | 3.142 | 0.461 | | 57.526 | | | 1.25 | |
| August 22, 2006 | ALOS 30 | 3.035 | 0.333 | 118.000 | 127.476 | 129.249 | 1.00 | 1.00 | 1.00 |
| | ASTER 30 | 3.071 | 0.325 | | 129.070 | | | 1.00 | |
| | SRTM 30 | 3.071 | 0.320 | | 130.919 | | | 1.00 | |
| | SRTM 90 | 3.142 | 0.317 | | 129.531 | | | 1.00 | |

The dependence of IUH on velocity has serious implications in the estimation of the peak flow and time peak of storms when using the UH approach [10, 21]. This reality became clear in the direct runoff prediction process as a result of the dynamic velocity, V being extremely sensitive to small changes in n_m , which was also proven by others [4, 10, 28]: thereupon the GIUH-Nash model performance [11]. Thus, it seems that n_m representing the site under consideration must be obtained prior to the use of the selected model for practical applications. In the SAGA-based stream networks, two main channels having the same stream order converged near the outlet resulting in a smaller length, L_Ω of higher orders as shown in Table 2. These values lead to poor correlation among the number of streams and the log-transformed mean stream length resulting R_L to be smaller than the minimum threshold values suggested by Rodriguez [21]. Eventually, K being a function of V , L_Ω and Horton's ratios, its results were also significantly affected. Conversely, GRASS-based Nash parameters are higher and Horton's ratios within the recommended ranges [21] due to higher, L_Ω . Table 4 shows the dynamic velocity and scale parameter of the different storm sand DEMs. The values of the dynamic velocity, ranging between 5 to 9 ms⁻¹, are high due to large main channel slopes (1.16 %) and mainly small value of n_m . Small value of K (< 0.5 h) is indicative of lower storage capacity of the catchment.

The quality of GIUH-Nash model-based runoff depends on the accuracy of the estimation of its parameters. Table 5 shows GRASS-based values of Nash parameters, peak runoff and time peak of different storms and DEMs. The implications of the adopted algorithms and corresponding Nash parameters on the predicted hydrographs were analyzed. Visual inspections of observed and predicted runoffs indicate that GRASS-based parameters give better results, as expected, than SAGA-based. The GRASS-based predicted hydrographs from all the DEM-scenarios are plotted in the same graph for visual comparison (Figure 8). The comparison reveals that the characteristics of the predicted hydrographs from the four DEM-scenarios are nearly in perfect match. Thus, we felt that there is no need to apply goodness of fit functions and statistical indices to each DEM-scenario. Rather, we opted to calculate predicted runoff averages (Q_{avg}) of the four DEM-scenarios and compare them with the observed hydrographs (Figure 9). It can be observed that Q_{avg} is larger than Q_o in three storm events, smaller in one storm event and nearly the same for the remaining one event. The time peaks are small (~ 1.0 h) due to smaller values of scale parameter. The predicted peak runoff averages have a time lag of 0.25 h.

On the other hand, the SAGA-based predicted hydrographs reveal significant mismatch with the observed hydrographs. The effects of lower values of Nash parameters from this algorithm are clearly revealed on the outputs. Poor prediction was obtained from the lower resolution DEMs (Figure 10) and relatively better estimate was obtained from SRTM 90. Figure 10 shows inconsistencies among predicted runoffs from the same storm event: there are over-prediction and under-prediction of the hydrograph characteristics. The lower values of n and K in most DEM-scenarios produced a short time peak (0.5 h) and time base (1.0 h) with the exception of SRTM 90 m. Table 6 shows SAGA-based Nash parameters, peak runoff and time peak. The estimated predicted peak runoffs are found to be different for all the DEM-scenarios.

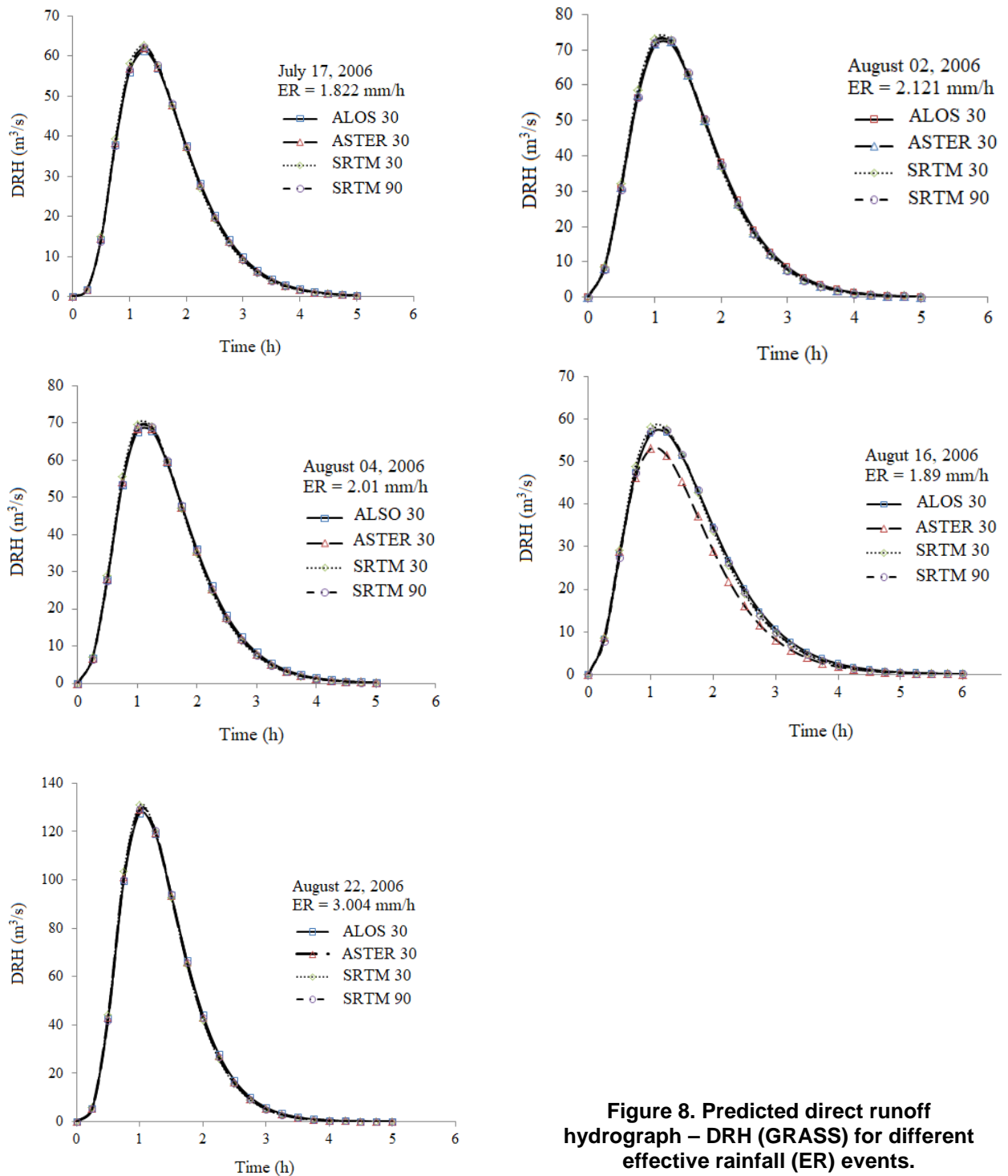


Figure 8. Predicted direct runoff hydrograph – DRH (GRASS) for different effective rainfall (ER) events.

The statistical measures of the selected model based on the two algorithms (Table 7 and Table 8) are obtained using equations 12–18. The various statistical analyses show GRASS-based approach is fitting better for the catchment under consideration than SAGA-based approach. For GRASS (Table 7), the minimum values of NSE and SC are 0.507 and 0.843, respectively, demonstrating the sufficiency of the GIUH-Nash model [39]. In general, the EV and ETP do not show significant variation among predicted and observed values. The negative values in REP, EV and ETP represent the predicted peak runoffs, volumes and corresponding time peaks are more than observed peak runoffs, volumes and time peaks. RMSE happens to be higher in some of the storm events.

On the other hand, the statistical indices of SAGA-based approach (Table 8) indicate that for the majority of the DEM-scenarios and storm events, the performance of GIUH-Nash is found to be unsatisfactory. The vast majority of NSE values are <0 ; hence, the residual variance is greater than the variance of the observed data indicating unacceptable model performance [39]. The values of the other indices are also considerably higher than that of GRASS-based model. Hydrograph characteristics of the lower resolution DEM-based predictions are smaller than observed values. As pointed out earlier in the preceding discussions, the reason for this approach poor performance is mainly associated with the smaller lengths of the higher orders.

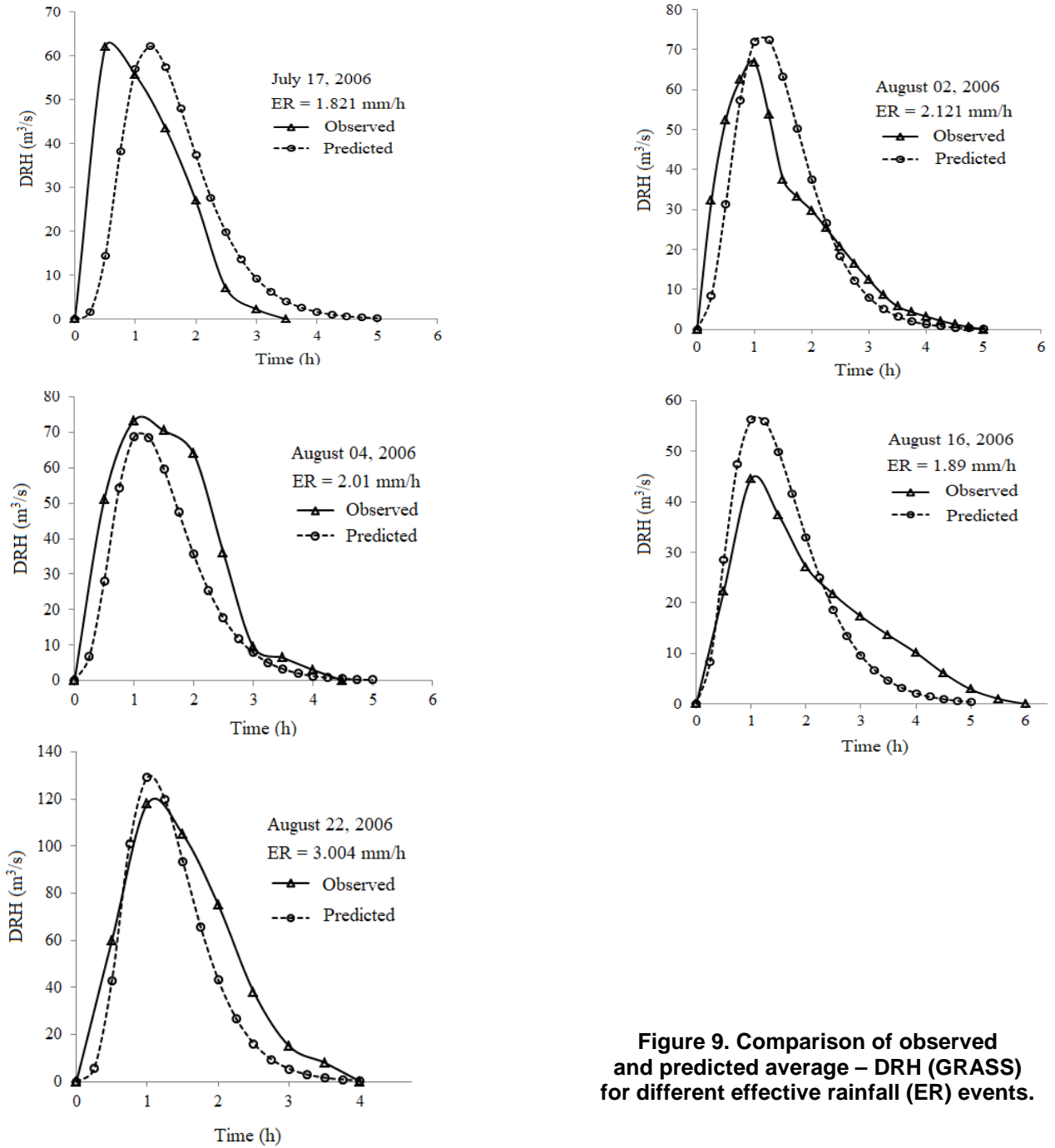


Figure 9. Comparison of observed and predicted average – DRH (GRASS) for different effective rainfall (ER) events.

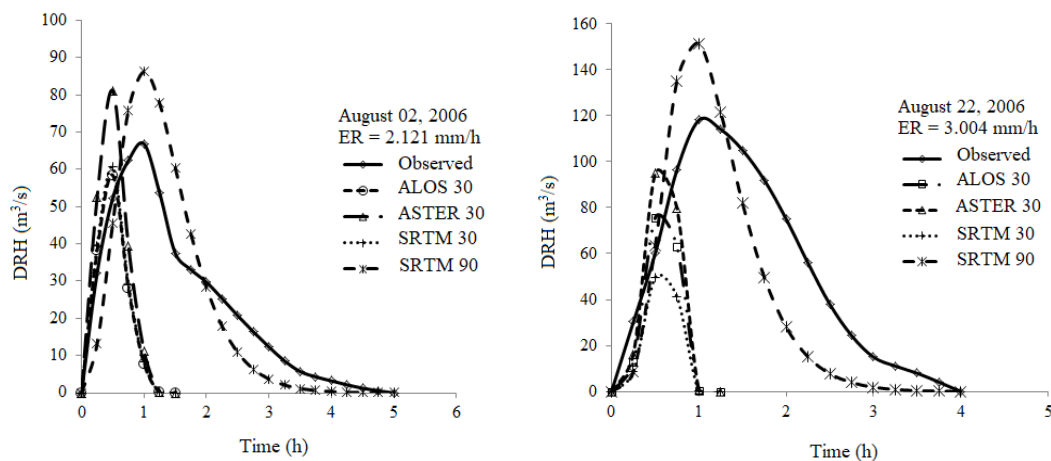


Figure 10. Examples of predicted and observed DRH (SAGA) comparisons.

Table 6. SAGA-based values of Nash parameters, peak runoff and time peak.

| Storm event | DEM | Nash parameters | | Peak runoff | | Time peak | |
|-----------------|----------|-----------------|--------|------------------|------------------|-----------|----------|
| | | n | K, h | Q_0, m^3s^{-1} | Q_p, m^3s^{-1} | T_0, h | T_p, h |
| July 17, 2006 | ALOS 30 | 2.938 | 0.052 | 61.921 | 88.528 | 1.00 | 0.50 |
| | ASTER 30 | 2.952 | 0.056 | | 100.791 | | 0.50 |
| | SRTM 30 | 2.975 | 0.046 | | 68.747 | | 0.50 |
| | SRTM 90 | 3.049 | 0.352 | | 72.837 | | 1.00 |
| August 02, 2006 | ALOS 30 | 2.938 | 0.043 | 66.860 | 58.453 | 1.00 | 0.50 |
| | ASTER 30 | 2.952 | 0.052 | | 81.101 | | 0.50 |
| | SRTM 30 | 2.975 | 0.043 | | 60.583 | | 0.50 |
| | SRTM 90 | 3.049 | 0.331 | | 86.277 | | 0.50 |
| August 04, 2006 | ALOS 30 | 2.938 | 0.050 | 73.301 | 91.633 | 1.00 | 0.50 |
| | ASTER 30 | 2.952 | 0.054 | | 106.070 | | 0.50 |
| | SRTM 30 | 2.975 | 0.044 | | 69.353 | | 0.50 |
| | SRTM 90 | 3.049 | 0.339 | | 82.971 | | 1.00 |
| August 16, 2006 | ALOS 30 | 2.938 | 0.051 | 44.585 | 92.258 | 1.00 | 0.50 |
| | ASTER 30 | 2.952 | 0.063 | | 129.356 | | 0.50 |
| | SRTM 30 | 2.975 | 0.052 | | 94.357 | | 0.50 |
| | SRTM 90 | 3.049 | 0.396 | | 43.720 | | 0.50 |
| August 22, 2006 | ALOS 30 | 2.938 | 0.040 | 118.000 | 75.537 | 1.00 | 0.50 |
| | ASTER 30 | 2.952 | 0.043 | | 94.868 | | 0.50 |
| | SRTM 30 | 2.975 | 0.036 | | 49.600 | | 0.50 |
| | SRTM 90 | 3.049 | 0.272 | | 151.388 | | 1.00 |

Table 7. GRASS-based statistical measures of GIUH-Nash model.

| Storm event | REP (%) | RMSE | EV (%) | ETP(h) | MAE | NSE | SC |
|-----------------|---------|--------|--------|--------|--------|-------|-------|
| July 17, 2006 | -0.349 | 16.237 | 0.742 | 0.75 | 10.375 | 0.507 | 0.843 |
| August 02, 2006 | -8.226 | 10.904 | -0.372 | 0.25 | 7.122 | 0.740 | 0.856 |
| August 04, 2006 | 6.335 | 14.013 | 30.101 | 0.00 | 10.132 | 0.759 | 0.948 |
| August 16, 2006 | -26.164 | 7.163 | 0.659 | 0.00 | 5.949 | 0.722 | 0.942 |
| August 22, 2006 | -1.498 | 16.561 | 21.501 | -0.25 | 13.319 | 0.840 | 0.967 |

Table 8. SAGA-based statistical measures of GIUH-Nash model.

| Storm event | DEM | REP (%) | RMSE | EV (%) | ETP | MAE | NSE | SC |
|-----------------|----------|----------|--------|--------|-------|--------|--------|-------|
| July 17, 2006 | ALOS 30 | -42.969 | 24.530 | 55.278 | 0.00 | 16.450 | -0.098 | 0.633 |
| | ASTER 30 | -62.773 | 25.670 | 48.541 | 0.00 | 17.539 | -0.203 | 0.587 |
| | SRTM 30 | -11.024 | 23.850 | 65.675 | 0.00 | 14.769 | -0.038 | 0.659 |
| | SRTM 90 | -17.629 | 15.118 | -0.039 | 0.50 | 9.011 | 0.583 | 0.879 |
| August 02, 2006 | ALOS 30 | 12.574 | 24.523 | 71.676 | -0.50 | 17.140 | -0.316 | 0.608 |
| | ASTER 30 | -21.300 | 24.627 | 60.547 | -0.50 | 18.189 | -0.327 | 0.604 |
| | SRTM 30 | 9.388 | 24.465 | 70.635 | -0.50 | 17.241 | -0.310 | 0.611 |
| | SRTM 90 | -29.041 | 11.095 | -1.142 | 0.00 | 8.281 | 0.731 | 0.933 |
| August 04, 2006 | ALOS 30 | -25.009 | 40.529 | 70.846 | -0.50 | 29.911 | -0.745 | 0.390 |
| | ASTER 30 | -44.705 | 41.371 | 66.076 | -0.50 | 30.598 | -0.818 | 0.342 |
| | SRTM 30 | 5.386 | 39.958 | 78.058 | -0.50 | 28.774 | -0.696 | 0.420 |
| | SRTM 90 | -13.191 | 16.396 | 29.496 | 0.00 | 11.783 | 0.714 | 0.928 |
| August 16, 2006 | ALOS 30 | -106.927 | 21.204 | 99.986 | -0.50 | 16.264 | -1.029 | 0.021 |
| | ASTER 30 | -190.133 | 21.171 | 99.890 | -0.50 | 16.248 | -1.023 | 0.059 |
| | SRTM 30 | -111.633 | 21.204 | 99.984 | -0.50 | 16.263 | -1.029 | 0.022 |
| | SRTM 90 | 1.939 | 13.822 | 71.180 | -0.50 | 11.578 | 0.138 | 0.758 |
| August 22, 2006 | ALOS 30 | 35.986 | 58.984 | 82.052 | -0.50 | 42.710 | -0.405 | 0.415 |
| | ASTER 30 | 19.603 | 58.953 | 77.381 | -0.50 | 42.658 | -0.404 | 0.416 |
| | SRTM 30 | 57.966 | 59.998 | 88.254 | -0.50 | 43.973 | -0.454 | 0.378 |
| | SRTM 90 | -28.295 | 25.457 | 20.932 | 0.00 | 20.186 | 0.738 | 0.920 |

4. Conclusions

Conclusions inferred from this study may be summarized in the following statements.

1. Despite in congruencies among physical and geographical parameters and elevation profiles derived from various DEMs, results of the study for the catchment Debarwa indicate that their implications on runoff predictions based on GIUH-Nash model are negligible unlike TOPMODEL [35] and SWAT [36, 37].

2. Algorithm selection affects the performance of the model in agreement with the works of [32, 33, 38]. GRASS algorithm generates hydrographs with reasonable accuracy to recorded hydrographs whereas SAGA-algorithm based model performance is found to be unsatisfactory. The authors conclude that care should be taken while selecting stream network generating algorithms for catchments similar to the Debarwa catchment, which have an outlet located near an upstream confluence of two major rivers.

3. Source and resolution of DEM insignificantly affects GIUH-Nash model performance as compared to algorithm selection. As such, GRASS-based runoff predictions are less influenced by source and resolution of DEM than SAGA-based. In this regard, lower resolution yields relatively consistent and acceptable performance than higher resolution which complies with the conclusions drawn by [37].

4. Considering the simplicity of the GIUH-Nash model development and application for practical purposes, ease of access to DEM and processing tools, good agreement of the theoretical and practical results from carefully chosen algorithms and consistency in the model outputs due to its inconsiderable dependence on source and resolution of DEM, the model has the potential to be a useful tool in resolving runoff prediction based difficulties in data scarce regions such as the Debarwa catchment in Eritrea.

5. Finally, in order to take a broad view of the findings of this study and promote the use of effective and appropriate runoff prediction approaches in ungauged catchments, future investigations should be undertaken in conjunction with available reference information systems. These investigations will include the GIUH-Nash model applicability and reliability in different agro-ecological zones, comparison of the selected model performance with other conventional and contemporary models and effects of DEM source and resolution and stream networks generating algorithm selection on the performance of various models in different catchment sin the territory of Eritrea.

References

1. FAO. Review of Water Resources by Country water reports 23. Rome. 2003. 79 p. [Online] URL: http://www.fao.org/nr/water/aquastat/countries_regions/ERI
2. Anghesom, A.G., Amlesom, S., Bovas, J.J.L. An overview of Eritrea's water resources. *International Journal of Engineering Research and Development*. 2017. Vol. 13. No. 3. Pp. 74–84.
3. Anghesom, A.G, Mathur B.S. Geomorphologic instantaneous unit hydrographs for rivers in Eritrea (East Africa). *Journal of Indian Water Resources Society*. 2014. Vol. 34. No. 1. Pp. 1–14.
4. Garry, L. Grabow, P., McCornick, G., James, R.G. Stream gauging of torrential rivers of eastern Eritrea. *Journal of Hydrologic Engineering*. 1998. Vol. 3. No. 3. Pp. 211–214.
5. Beven, K.J. *Rainfall-Runoff Modelling: The Primer*, John Wiley and sons Ltd. 2012. Pp. 25–49.
6. Singh, V.P. *Hydrologic Systems: Rainfall-Runoff Modeling vol. I*. Prentice-Hall, Englewood Cliffs. New Jersey. 1988.
7. Sherman, L.K. Streamflow from rainfall by unit-graph method. *Engineering news-Record*. 1932. Vol. 108. No. 4. Pp. 501–505.
8. Hawker, L., Bates, P., Neal, J., Rougier, J. Perspectives on digital elevation model (DEM) simulation for flood modeling in the absence of a high-accuracy open access global DEM. *Frontiers in Earth Science*. 2018. Vol. 6. No. 233. doi.org/10.3389/feart.2018.00233.
9. Sarkar, S., Goel, N.K., Mathur, B.S. Adequacy of Nakagami-m distribution function to derive GIUH. *Journal of Hydrologic Engineering*. 2009. Vol. 14. No. 10. Pp. 1070–1079.
10. Kumar, R., Chatterjee, C., Singh, R.D., Lohani, A.K., Kumar, S. Runoff estimation for ungauged catchments using GIUH. *Hydrologic Processes*. 2007. Vol. 21. No. 4. Pp. 1829–1840.
11. Dooge, J.C.I. A general theory of unit hydrograph. *Journal of Geophysical Research*. 1959. Vol. 64. No. 2. Pp. 241–256.
12. Snyder, F.F. Synthetic unit hydrographs. *Transactions of the American Geophysical Union*. 1938. Vol. 19. No. 1. Pp. 447–454.
13. Pilgrim, D.H., Cordery, I., Maidment, D.R. at al. Flood Runoff in Maidment D.R.(Eds.). *Handbook of Hydrology*. McGraw Hill. New York, 1993. 9.27 p.
14. Gupta, V.K., Waymire, E.C., Wang, C.T. A representation of an instantaneous unit hydrograph from geomorphology. *Water Resources Research*. 1980. Vol. 16. No. 5. Pp. 855–862.
15. Clark, C.O. Storage and the unit hydrograph. *Transactions. American Society of Civil Engineers*. 1945. Vol. 110. No. 1. Pp. 1419–1446.
16. Nash, J.E. Determining runoff from rainfall. *Proceedings of the institution of civil engineers*. Dublin. 1958. Vol. 10. Pp. 163–84.
17. Nash, J.E. The form of the instantaneous unit hydrograph. *International Association of Scientific Hydrology Publication*. 1957. Vol. 45. No. 3. Pp. 114–121.
18. Yen, B.C., Lee, K.T. Unit hydrograph derivation for ungauged watersheds by stream order laws. *Journal of Hydrologic Engineering*. 1997. Vol. 2. No. 1. Pp. 1–9.
19. Nourani, V., Singh, V.P. Delafrouz, D. Three geomorphological rainfall-runoff models based on the linear reservoir concept. *Journal of Catena*. 2008. Vol. 76. No. 3. Pp. 206–214.
20. Rodriguez-Iturbe, I., Valdes, J.B. The geomorphologic structure of hydrology response. *Water Resources Research*. 1979. Vol. 15. No. 6. Pp. 1409–1420.
21. Horton, R.E. Erosional development of streams and their drainage basins: hydrophysical approach to quantitative morphology. *Geological Society of America Bulletin*. 1945. Vol. 56. Pp. 275–370
22. Strahler, A.N. Quantitative analysis of watershed geomorphology. *Transactions American Geophysical Union*. 1957. Vol. 38. No. 6. Pp. 913–920.
23. Gupta, V.K., Waymire, E.C., Rodriguez-Iturbe, I. On scales gravity and network structure in basin runoff. In: Gupta, V.K., Rodriguez-Iturbe, I., Wood, E.F. (Eds.), *Scale Problems in Hydrology*. D. Reidel, Dordrecht, Holland. 1986. Pp. 159–184.
24. Rodriguez-Iturbe, I., Gonzalez-Sanabria, M., Bras, R.L. The geomorphoclimatic theory of the instantaneous unit hydrograph. *Water Resources Research*. 1982a. Vol. 18. No. 4. Pp. 877–886.
25. Rosso, R. Nash model relation to Horton order ratios. *Water Resources Research*. 1984. Vol. 20. No. 7. Pp. 914–920.
26. Lee, K.T., Yen, B.C. Geomorphology and kinematic-wave-based hydrograph derivation. *Journal of Hydraulic Engineering*. 1997. Vol. 123. No. 1. Pp. 73–80.

27. Bhaskar, N.R., Parida, B.P., Nayak, A.K. Flood estimation for ungauged catchments using the GIUH. *Journal of Water Resources Planning and Management*. 1997. Vol. 123. No. 4. Pp. 228–238.
28. Choi, Y.J., Lee, G., Kim J.C. Estimation of the Nash model parameters based on the concept of geomorphologic dispersion. *Journal of Hydrologic Engineering*. 2011. Vol. 16. No. 11. Pp. 806–817.
29. Zakizadeh, F., Malekinezhad, H. Comparison of methods for estimation of flood hydrograph characteristics. *Meteorology and Hydrology*. 2015. Vol. 40. No.12. Pp. 74–86. (rus)
30. Guzha, A.C., Hardy, T.B. Simulating streamflow and water table depth with a coupled hydrological model. *Water Science and Engineering*. 2010. Vol. 3. No. 3.Pp. 241–256.
31. Wechsler, S.P. Uncertainties associated with digital elevation models for hydrologic applications: a review. *Hydrology and Earth Systems Sciences Discussions, European Geosciences Union*. 2006, Vol. 3. No. 4. Pp. 2343–2384.
32. Wechsler, S.P. Perceptions by digital elevation model uncertainty by DEM users. *URISA Journal*. 2003. Vol. 15. No. 2. Pp. 57–64.
33. Bolstad, P., Stowe, T. An evaluation of DEM accuracy: elevation, slope, and aspect. *Photogrammetric Engineering and Remote Sensing*. 1994. Vol. 60. No. 11. Pp. 1327–1332.
34. Wolock, D., Price, C. Effect of digital elevation model map scale and data resolution on a topography-based watershed model. *Water Resources Research*. 1994. Vol. 30. No. 11. Pp. 3041–3052.
35. Chapplot, V. Impact of DEM mesh size and soil map scale on SWAT runoff, sediment, and NO₃-N loads predictions. *Journal of Hydrology*. 2005. Vol. 312 No. 1–4. Pp. 207–222.
36. Reddy, S.A., Reddy, J.M. Evaluating the influence of spatial resolutions of DEM on watershed runoff and sediment yield using SWAT. *Journal of Earth System Science*. 2015. Vol. 124. No. 7. Pp. 1517–1529.
37. Azizian, A., Shokoohi, A. DEM resolution and stream delineation threshold effects on the results of geomorphologic-based rainfall runoff models. *Turkish Journal of Engineering and Environmental Sciences*. 2014. Vol. 38. Pp. 64–78.
38. Nash, J.E., Sutcliffe, J.V. River flow forecasting through conceptual models part I: a discussion of principles. *Journal of Hydrology*. 1970. Vol. 10. No. 3. Pp. 282–290.

Contacts:

Dmitry Kozlov, +79854813569; kozlovdv@mail.ru

Anghesom Alemngus Ghebrehiwot, +79851936320; bahghi2012@gmail.com

© Kozlov, D.V., Ghebrehiwot, A.A., 2019



DOI: 10.18720/MCE.87.9

Эффективность цифровых моделей рельефа и моделей Нэша в прогнозировании стока

Д.В. Козлов*, А.А. Гебрехиwот,

*Национальный исследовательский Московский государственный строительный университет,
г. Москва, Россия*

* E-mail: kozlovdv@mail.ru

Ключевые слова: цифровая модель рельефа, ГИС-алгоритм, модель GIUH-Nash, прямой поверхностный сток, гидрограф, водосбор, речная сеть, прогноз стока.

Аннотация. Цифровые модели рельефа (ЦМР) широко используются в гидрологическом моделировании и определении геоморфологических свойств водосборных бассейнов. В последнее время гидрологи проявляют интерес к изучению воздействия ЦМР из различных источников на моделируемые результаты. В рамках этих усилий данное исследование было направлено на оценку влияния различных ЦМР и выбора алгоритмов прогноза геоморфологических мгновенных единичных гидрографов (GIUH) прямого поверхностного стока на основе модели Нэша для неизученного речного водосбора Дебарва в Эритрее. Были применены четыре ЦМР с открытым исходным кодом и два алгоритма квантовой географической информационной системы (QGIS) (GRASS и SAGA), а соответствующие результаты были оценены с использованием пяти наблюдаемых паводковых событий. Эти два алгоритма привели к созданию речных сетей с одинаковыми порядками русел, но различными геоморфологическими характеристиками, такими как соотношение русел. Субъективная и объективная оценки результатов указали на то, что эффективность модели, основанной на SAGA, была неудовлетворительной, в то время как модель GIUH-Nash, основанная на алгоритме GRASS, была приемлемой для всех сценариев ЦМР, независимо от их источников и разрешений. В исследовании сделан вывод о том, что выбор ЦМР при расчете гидрографов стока для условий водосбора Дебарва мало влияет на прогнозы прямого поверхностного стока на основе модели GIUH-Nash. Однако при выборе алгоритмов генерации речной сети следует проявлять большую осторожность, особенно для водосборных бассейнов, выходы которых расположены вблизи слияния двух крупных рек.

Литература

1. FAO. Review of Water Resources by Country water reports 23. Rome. 2003. 79 p. [Электронный ресурс] URL: http://www.fao.org/nr/water/aquastat/countries_regions/ERI
2. Anghesom A.G., Amlesom S., Bovas J.J.L. An overview of Eritrea's water resources // International Journal of Engineering Research and Development. 2017. Vol. 13. № 3. Pp. 74–84.
3. Anghesom A.G., Mathur B.S. Geomorphologic instantaneous unit hydrographs for rivers in Eritrea (East Africa) // Journal of Indian Water Resources Society. 2014. Vol. 34. № 1. Pp. 1–14.
4. Garry L., Grabow P., McCornick G., James, R.G. Stream gauging of torrential rivers of eastern Eritrea // Journal of Hydrologic Engineering. 1998. Vol. 3. № 3. Pp. 211–214.
5. Beven K.J. Rainfall-Runoff Modelling: The Primer, John Wiley and sons Ltd. 2012. Pp. 25–49.
6. Singh V.P. Hydrologic Systems: Rainfall-Runoff Modeling vol. I. Prentice-Hall, Englewood Cliffs. New Jersey. 1988.
7. Sherman L.K. Streamflow from rainfall by unit-graph method // Engineering news-Record. 1932. Vol. 108. № 4. Pp. 501–505.
8. Hawker L., Bates P., Neal J., Rougier J. Perspectives on digital elevation model (DEM) simulation for flood modeling in the absence of a high-accuracy open access global DEM // Frontiers in Earth Science. 2018. Vol. 6. № 233. doi.org/10.3389/feart.2018.00233.
9. Sarkar S., Goel N.K., Mathur B.S. Adequacy of Nakagami-m distribution function to derive GIUH // Journal of Hydrologic Engineering. 2009. Vol. 14. № 10. Pp. 1070–1079.
10. Kumar R., Chatterjee C., Singh R.D., Lohani A.K., Kumar S. Runoff estimation for ungauged catchments using GIUH // Hydrologic Processes. 2007. Vol. 21. № 4. Pp. 1829–1840.
11. Dooge J.C.I. A general theory of unit hydrograph // Journal of Geophysical Research. 1959. Vol. 64. № 2. Pp. 241–256.
12. Snyder F.F. Synthetic unit hydrographs // Transactions of the American Geophysical Union. 1938. Vol. 19. № 1. Pp. 447–454.
13. Pilgrim D.H., Cordery I., Maidment D.R. at al. Flood Runoff in Maidment D.R. (Eds.). Handbook of Hydrology. McGraw Hill. New York, 1993. 9.27 p.

14. Gupta V.K., Waymire E.C., Wang C.T. A representation of an instantaneous unit hydrograph from geomorphology // *Water Resources Research*. 1980. Vol. 16. № 5. Pp. 855–862.
15. Clark C.O. Storage and the unit hydrograph. *Transactions // American Society of Civil Engineers*. 1945. Vol. 110. № 1. Pp. 1419–1446.
16. Nash J.E. Determining runoff from rainfall. *Proceedings of the institution of civil engineers*. Dublin. 1958. Vol. 10. Pp. 163–84.
17. Nash J.E. The form of the instantaneous unit hydrograph // *International Association of Scientific Hydrology Publication*. 1957. Vol. 45. № 3. Pp. 114–121.
18. Yen B.C., Lee K.T. Unit hydrograph derivation for ungauged watersheds by stream order laws // *Journal of Hydrologic Engineering*. 1997. Vol. 2. № 1. Pp. 1–9.
19. Nourani V., Singh V.P., Delafrouz D. Three geomorphological rainfall–runoff models based on the linear reservoir concept // *Journal of Catena*. 2008. Vol. 76. № 3. Pp. 206–214.
20. Rodriguez-Iturbe I., Valdes J.B. The geomorphologic structure of hydrology response. *Water Resources Research*. 1979. Vol. 15. № 6. Pp. 1409–1420.
21. Horton R.E. Erosional development of streams and their drainage basins: hydrophysical approach to quantitative morphology // *Geological Society of America Bulletin*. 1945. Vol. 56. Pp. 275–370
22. Strahler A.N. Quantitative analysis of watershed geomorphology // *Transactions American Geophysical Union*. 1957. Vol. 38. № 6. Pp. 913–920.
23. Gupta V.K., Waymire E.C., Rodriguez-Iturbe I. On scales gravity and network structure in basin runoff // Gupta V.K., Rodriguez-Iturbe I., Wood E.F. at al. *Scale Problems in Hydrology*. D. Reidel, Dordrecht, Holland. 1986. Pp. 159–184.
24. Rodriguez-Iturbe I., Gonzalez-Sanabria M., Bras R.L. The geomorphoclimatic theory of the instantaneous unit hydrograph // *Water Resources Research*. 1982a. Vol. 18. № 4. Pp. 877–886.
25. Rosso R. Nash model relation to Horton order ratios // *Water Resources Research*. 1984. Vol. 20. № 7. Pp. 914–920.
26. Lee K.T., Yen B.C. Geomorphology and kinematic-wave-based hydrograph derivation // *Journal of Hydraulic Engineering*. 1997. Vol. 123. № 1. Pp. 73–80.
27. Bhaskar N.R., Parida B.P., Nayak A.K. Flood estimation for ungauged catchments using the GIUH // *Journal of Water Resources Planning and Management*. 1997. Vol. 123. № 4. Pp. 228–238.
28. Choi Y.J., Lee G., Kim J.C. Estimation of the Nash model parameters based on the concept of geomorphologic dispersion // *Journal of Hydrologic Engineering*. 2011. Vol. 16. № 11. Pp. 806–817.
29. Zakizadeh F., Malekinezhad H. Comparison of methods for estimation of flood hydrograph characteristics // *Meteorology and Hydrology*. 2015. Vol. 40. №12. Pp. 74–86.
30. Guzha A.C., Hardy T.B. Simulating streamflow and water table depth with a coupled hydrological model // *Water Science and Engineering*. 2010. Vol. 3. № 3.Pp. 241–256.
31. Wechsler, S.P. Uncertainties associated with digital elevation models for hydrologic applications: a review. *Hydrology and Earth Systems Sciences Discussions, European Geosciences Union*. 2006, Vol. 3. № 4. Pp. 2343–2384.
32. Wechsler S.P. Perceptions by digital elevation model uncertainty by DEM users // *URISA Journal*. 2003. Vol. 15. № 2. Pp. 57–64.
33. Bolstad P., Stowe T. An evaluation of DEM accuracy: elevation, slope, and aspect // *Photogrammetric Engineering and Remote Sensing*. 1994. Vol. 60. № 11. Pp. 1327–1332.
34. Wolock D., Price C. Effect of digital elevation model map scale and data resolution on a topography-based watershed model // *Water Resources Research*. 1994. Vol. 30. № 11. Pp. 3041–3052.
35. Chapplot V. Impact of DEM mesh size and soil map scale on SWAT runoff, sediment, and NO₃-N loads predictions // *Journal of Hydrology*. 2005. Vol. 312 № 1–4. Pp. 207–222.
36. Reddy S.A., Reddy J.M. Evaluating the influence of spatial resolutions of DEM on watershed runoff and sediment yield using SWAT // *Journal of Earth System Science*. 2015. Vol. 124. № 7. Pp. 1517–1529.
37. Azizian A., Shokoohi A. DEM resolution and stream delineation threshold effects on the results of geomorphologic-based rainfall runoff models. *Turkish Journal of Engineering and Environmental Sciences*. 2014. Vol. 38. Pp. 64–78.
38. Nash J.E., Sutcliffe J.V. River flow forecasting through conceptual models part I: a discussion of principles // *Journal of Hydrology*. 1970. Vol. 10. № 3. Pp. 282–290.

Контактные данные:

Дмитрий Вячеславович Козлов, +79854813569; эл. почта: kozlovdv@mail.ru
Анхесом Алемнугс Гебрехивот, +79851936320; эл. почта: bahghi2012@gmail.com